Assessing the effects of LXR agonists on cellular cholesterol handling: a stable isotope tracer study

Karpagam Aravindhan,* Christine L. Webb,† Michael Jaye,† Avijit Ghosh,* Robert N. Willette,† N. John DiNardo,* and Beat M. Jucker[1,†]

Department of Applied Physics,* College of Arts and Sciences, Drexel University, Philadelphia, PA 19104; and Cardiovascular and Urogenital Center of Excellence in Drug Discovery,† GlaxoSmithKline, King of Prussia, PA 19406

Abstract The liver X receptors (LXRs) α and β are responsible for the transcriptional regulation of a number of genes involved in cholesterol efflux from cells and therefore may be molecular targets for the treatment of cardiovascular disease. However, the effects of LXR ligands on cholesterol turnover in cells has not been examined comprehensively. In this study, cellular cholesterol handling (e.g., synthesis, catabolism, influx, and efflux) was examined using a stable isotope labeling study and a two-compartment modeling scheme. In HepG2 cells, the incorporation of ^{13}C into cholesterol from [1-^{13}C]acetate was analyzed by mass isotopomer distribution analysis in conjunction with nonsteady state, multicompartment kinetic analysis to calculate the cholesterol fluxes. Incubation with synthetic, nonsteroidal LXR agonists (GW3965, T0901317, and SB742881) increased cholesterol synthesis (~10-fold), decreased cellular cholesterol influx (71–82%), and increased cellular cholesterol efflux (1.7- to 1.9-fold) by 96 h. As a consequence of these altered cholesterol fluxes, cellular cholesterol decreased (36–39%) by 96 h. The increased cellular cholesterol turnover was associated with increased expression of the LXR-activated genes ABCA1, ABCG1, FAS, and sterol-regulatory element binding protein 1c. In summary, the mathematical model presented allows time-dependent calculations of cellular cholesterol fluxes. These data demonstrate that all of the cellular cholesterol fluxes were altered by LXR activation and that the increase in cholesterol synthesis did not compensate for the increased cellular cholesterol efflux, resulting in a net cellular cholesterol loss.—Aravindhan, K., C. L. Webb, M. Jaye, A. Ghosh, R. N. Willette, N. J. Di Nardo, and B .M. Jucker. **Assessing the effects of LXR agonists on cellular cholesterol handling: a stable isotope tracer study. *J. Lipid Res.* 2006.** 47: **1250–1260.**

Supplementary key words liver X receptor • HepG2 • turnover • compartmental • mass isotopomer distribution analysis

The liver X receptor (LXR) is an oxysterol-sensing nuclear receptor responsible for transcriptional regulation of a number of genes involved in reverse cholesterol transport and therefore may be a molecular target for the treatment of cardiovascular disease (1–3). LXR is a member of the nuclear receptor family that regulates cellular cholesterol efflux (4) and whole body cholesterol excretion (5) and is endogenously activated by various oxysterols (6), including 24(*S*),25-epoxycholesterol and 22(*R*)-hydroxycholesterol, an intermediate in steroid hormone production (7, 8). Additionally, synthetic LXR agonists that potently upregulate macrophage ABCA1 expression have been shown to be antiatherogenic in genetic mouse models of atherosclerosis (9, 10).

Cellular cholesterol metabolism and handling has been examined in terms of its synthesis by measuring the fraction of newly synthesized cholesterol (11, 12), in terms of catabolism by measuring levels of bile acids through biochemical assays or HPLC (13, 14), in terms of influx by measuring the radioactivity of absorbed [^{3}H]cholesteryl oleate (15, 16), and in terms of efflux by measuring specific radioactivity in labeled cells (17–20). However, prior methods address only the unidirectional flow of cholesterol and are not capable of measuring the bidirectional flow of cholesterol. A comprehensive analysis of cholesterol turnover by assessing the bidirectional flow of cholesterol is critical when examining LXR activation. Therefore, the focus of this study was to investigate the kinetics of cholesterol synthesis and transport in/out of HepG2 cells after treatment with several classes of natural and synthetic LXR agonists, such as the nonsteroidal synthetic compounds GW3965, SB742881, and T0901317, the steroidal synthetic agonist *N,N*-dimethly-3β-hydroxy-cholenamide (DMHCA), and the natural steroidal agonists 22(*R*)-hydroxycholesterol and 24(*S*),25-epoxycholesterol. HepG2 cells were chosen for this study because this cell line is often used

Manuscript received 22 November 2005 and in revised form 9 March 2006.

Published, JLR Papers in Press, March 27, 2006.
DOI 10.1194/jlr.M500512-JLR200

Abbreviations: APE, atom percentage excess; apoB, apolipoprotein B; CYP7A1, cholesterol 7α-hydroxylase; DMHCA, *N,N*-dimethly-3β-hydroxy-cholenamide; LDLR, low density lipoprotein receptor; LXR, liver X receptor; MIDA, mass isotopomer distribution analysis; SR-BI, scavenger receptor class B type I; SREBP1c, sterol-regulatory element binding protein 1c.

[1] To whom correspondence should be addressed.
e-mail: beat_m_jucker@gsk.com

for cholesterol metabolic studies and has the constitutive ability to synthesize and secrete lipoproteins (21, 22). However, it is acknowledged that HepG2 cells differ from primary human hepatocytes in their production of bile acids, a catabolic product of cholesterol (23). LXR-regulated genes involved in reverse cholesterol transport and lipogenesis were also investigated to assess the temporal correlation of cholesterol flux with gene activation. Additionally, a HMG-CoA reductase inhibitor, atorvastatin, was used to examine the dynamic fidelity of the kinetic analysis and to compare its effects on cellular cholesterol handling with those observed with several classes of LXR agonist. We used [1-^{13}C] sodium acetate as a precursor for cholesterol synthesis, and mass isotopomer distribution analysis (MIDA) (24, 25) of the ^{13}C-labeled cholesterol molecule allowed for the precursor pool enrichment and fraction of newly synthesized cholesterol to be calculated. These parameters were then used to obtain cholesterol flux information using a two-compartment kinetic model.

EXPERIMENTAL PROCEDURES

Cell culture

HepG2 cells were cultured in DMEM supplemented with 10% FBS, penicillin (100 U/ml), streptomycin (100 μg/ml), high glucose (25 mM), sodium bicarbonate (45 mM), and GlutaMax® (2 mM). Cells were seeded at 5×10^5 per dish into 60 mm dishes 2 days before the start of the experiment. To avoid depleting the cells of the tracers or LXR agonists (whose concentration decreases by 60% within 24 h) and essential growth supplements, the cells were replenished with fresh medium and the tracer at appropriate concentrations every 24 h. Cellular toxicity was measured using the ToxiLight nondestructive cytotoxicity kit (No. LT17-217; Cambrex Bio Science, Inc., Rockland, ME). Total apolipoprotein B (apoB) secreted by the cells to the culture medium was analyzed using ELISA kit A70102 (AlerChek, Inc., Portland, ME).

[1-^{13}C]sodium acetate study

To measure cholesterol synthesis and to model cholesterol flux kinetics, HepG2 cells were seeded in 60 mm dishes at an optimal seeding density to become 80% confluent by day 2 after seeding. On the third day, cells were given fresh medium with [1-^{13}C]sodium acetate (10 mM) (Cambridge Isotope Laboratories, Inc., Andover, MA.), 99% isotope purity. The control groups received vehicle (0.1% DMSO, ethanol, or methanol), and the treatment group received GW3965, T0901317, or SB742881 (1 μM in DMSO), 22(*R*)-hydroxycholesterol, 24(*S*),25-epoxycholsterol, or DMHCA (1 μM in ethanol), or atorvastatin (1 μM in methanol). The cells were supplemented with medium containing LXR agonists or atorvastatin and [1-^{13}C]sodium acetate every 24 h for up to 4 days. The LXR agonist concentrations used were typical of efficacious plasma concentrations observed in hamsters after oral administration of drug at 10 mg/kg body weight (unpublished observation).

Cholesterol handling was also examined in the absence of serum with or without exogenous apoA-I. In these studies, cells were given 10% FBS on day 1 followed by serum-free medium with apoA-I on day 2. The treated group received GW3965 (1 μM) on both day 1 and day 2, and [1-^{13}C]acetate was administered to all groups on day 2. Therefore, treatment was for 48 h, whereas acetate incorporation was for 24 h.

Cholesterol extraction and derivatization

Total cholesterol, free cholesterol, cholesteryl ester, and other neutral sterols were extracted as described previously (11) with some modifications. Briefly, at the end of the treatment, cells were washed twice with ice-cold PBS. The cell culture medium was removed and stored at 4°C until analyzed. Cells were scraped into 2 ml of PBS and centrifuged at 1,000 rpm for 5 min. The PBS supernatant was discarded, and the cell pellets were saved at −80°C until analyzed. Cholesterol was extracted from the cell pellets twice with hexane-isopropanol (3:2, v/v), and 5α-cholestane was added as an internal recovery standard. The dried extract was saponified by adding freshly prepared 1 N KOH ethanolic solution (3 ml). Total cholesterol was derivatized as described previously (26). Recoveries for cholesterol and cholesteryl esters were assessed using cholesterol and cholesteryl oleate standards and found to range from 84% to 92%.

Analytical methods

An HP 5973 mass selective detector coupled with an HP 6890 gas chromatograph equipped with an HP-5 column (95% dimethylsiloxane) was used to measure cholesterol concentration and enrichment. The GC-MS apparatus was operated using splitless mode for higher sensitivity. In the scan-acquisition mode, dwell times were optimized for monitoring the internal standard peak at *m/z* 217 and the ^{13}C-labeled cholesterol species from *m/z* 367–382.

MIDA

The fraction of newly synthesized cholesterol in the cell and medium compartments and the fractional enrichment of the cholesterol precursor pool were obtained using MIDA (27). An in-house program that uses an unbiased simulation algorithm (Monte Carlo) was used to obtain the percentage of precursor ^{13}C enrichment and the percentage of newly synthesized cholesterol. The atom percentage excess (APE), a standard parameter used to measure ^{13}C enrichment, was converted to percentage of newly synthesized cholesterol using the validated technique of Hellerstein and colleagues (24, 25).

Multicompartment kinetic analysis

A multicompartment kinetic analysis was performed using SAAM II software, version 1.1.1 (SAAM Institute, Inc., Seattle, WA). This software allows for a simple and direct analysis of tracer kinetics using a compartment model approach. A precursor-product model was developed with a tracer (labeled) and a tracee (unlabeled) system. The notation F(destination, source) represents the total cholesterol flux measured as μg/h/mg cell protein. F(0,1) represents the cholesterol catabolic flux (i.e., bile acid synthesis, steroid synthesis, or other irreversible loss of cholesterol from the cells), F(1,2) represents the total cholesterol flux from the medium to the cells, and F(2,1) represents the total cholesterol flux from the cells to the medium. The administration of the [1-^{13}C]acetate precursor was treated as a function of the endogenous flux U(1) equivalent to the cholesterol synthesis flux (**Fig. 1**), corresponding to the fraction of precursor enrichment. In the experiments in which equilibrium was not impaired significantly [untreated controls, 22(*R*)-hydroxycholesterol], the size of the cell and medium cholesterol pools (pool 1 and pool 2, respectively) were considered constant, and in experiments in which the equilibrium was disturbed [GW3965, T0901317, SB742881, 24(*S*),25-epoxycholesterol, DMHCA groups (see Figs. 2, 3 below)], the actual cholesterol content of cells as well as medium was used in the SAAM II compartment analysis, as explained previously (28–30). Using the actual values of cellular

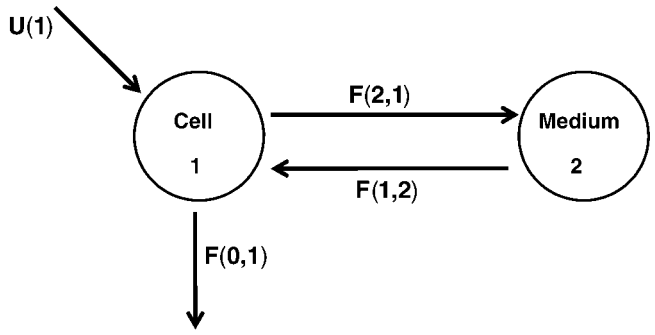

Fig. 1. Two-compartment kinetic model scheme. Compartment 1 represents the intracellular cholesterol pool, and compartment 2 represents the extracellular cholesterol pool. The associated fluxes are shown as F(destination, source). U(1) is the endogenous flux equivalent to the cholesterol synthesis flux. F(0,1) represents the cholesterol catabolic flux (i.e., bile acid synthesis, steroid synthesis, or other irreversible loss of cholesterol from the cells), F(1,2) represents the total cholesterol flux from the medium to the cells, and F(2,1) represents the total cholesterol flux from the cells to the medium.

and medium cholesterol allowed for the linear cumulative two-compartmental model to be investigated more explicitly. Replenishment of the cells with fresh medium including drug and tracer was accounted for in the model to provide a more accurate calculation.

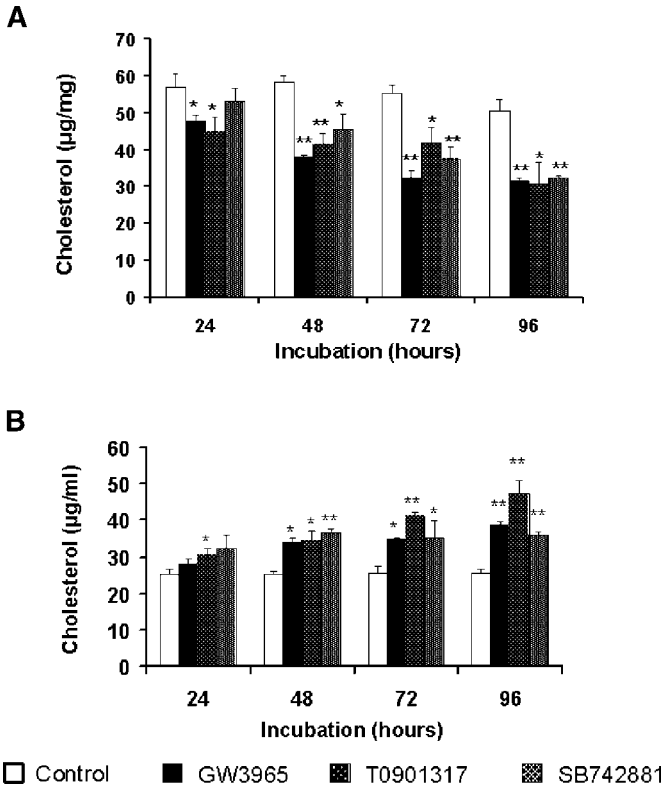

Fig. 2. Total cellular and culture medium cholesterol after treatment with nonsteroidal liver X receptor (LXR) agonists. Total cholesterol is shown in HepG2 cells (A) and in the culture medium (B) for up to 96 h of treatment with GW3965 (1 μM), T0901317 (1 μM), or SB742881 (1 μM). Data are presented as means ± SEM (n = 3). * $P < 0.01$, ** $P < 0.001$, control versus treated groups.

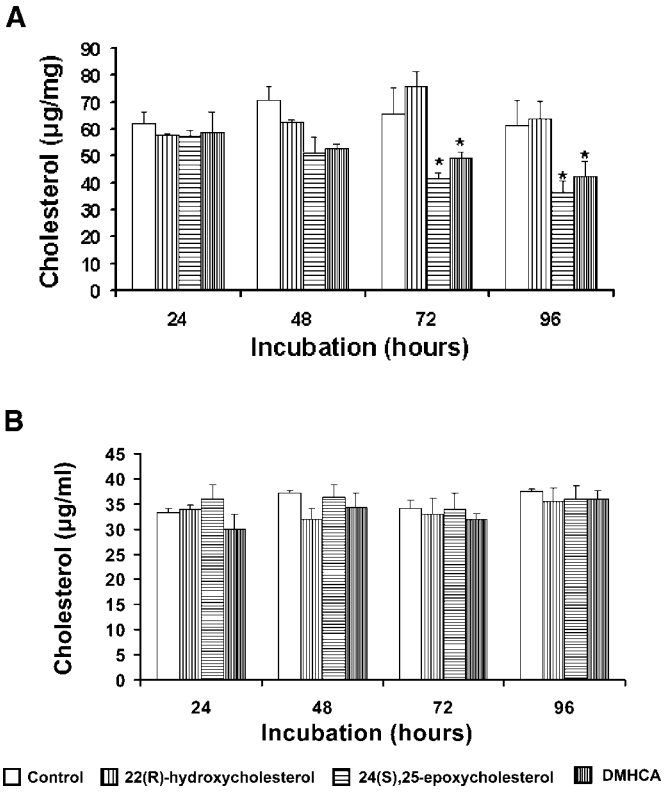

Fig. 3. Total cellular and culture medium cholesterol after treatment with steroidal LXR agonists. Total cholesterol is shown in HepG2 cells (A) and in the culture medium (B) for up to 96 h of treatment with 22(*R*)-hydroxycholesterol (1 μM), 24(*S*),25-epoxycholesterol (1 μM), or *N*,*N*-dimethly-3β-hydroxy-cholenamide (DMHCA; 1 μM). Data are presented as means ± SEM (n = 3). * $P < 0.05$, control versus treated groups.

Protein, RNA, and gene expression analysis

Cellular protein was measured using the Bio-Rad DC protein assay (Bio-Rad Laboratories, South San Francisco, CA) according to the manufacturer's instructions. Total RNA was isolated from HepG2 cells using the Qiagen RNeasy 96 kit (No. 74181; Qiagen, Valencia, CA). cDNA was then synthesized with random hexamer primers using the Superscript-III first-strand synthesis system for RT-PCR (No. 18080-051; Invitrogen Corp., Carlsbad, CA). Gene-specific quantitative PCR mixes were prepared using 50 ng of cDNA, 0.4 μM forward primer, 0.4 μM reverse primer, and 0.2 μM FAM-labeled fluorogenic probe (Applied Biosystems, Foster City, CA) to a reaction volume of 25 μl. Quantitative PCR was performed on an ABI PRISM® 7700 sequence detection system. The comparative cycle threshold method was used to quantitate gene expression in cells. Data are reported as fold change from control. All assays were performed in quadruplicate. The following primer and probe sets were used: hABCA1 forward, 5′-GCTCCCGGAGTTGTTGGAAA-3′; hABCA1 reverse, 5′-GTATAAAGAAGCCTCCGAGCATC-3′; hABCA1 probe, 6FAM-TTTAACAAATCCATTGTGGCTCGCCTGT-TAMRA; hABCG1 forward, 5′-AGCATCATGAGGGACTCGGT-3′; hABCG1 reverse, 5′-GGAGGCCGATCCCAATGT-3′; hABCG1 probe, 6FAM-CTGACACACCCTGCGCATCACCTCG-TAMRA; hFAS forward, 5′-ACCTGGGCGCGGACTAC-3′; hFAS reverse, 5′-CGATGACGTGGACGGATACTT-3′; hFAS probe, 6FAM-ACCTCTCCCAGGTATGCGACGGG-TAMRA. For the detection of human sterol-regulatory

element binding protein 1c (SREBP1c), HMG-CoA reductase, scavenger receptor class B type I (SR-BI), SREBP2, low density lipoprotein receptor (LDLR), and cholesterol 7α-hydroxylase (CYP7A1), commercial primer/probe sets Hs00231674_ml, Hs00168352_ml, Hs00194092_ml, Hs00190237_ml, Hs00181192_ml, and Hs00167982_ml, respectively, were used (Assays by Demand; Applied Biosystems).

Statistical analysis

All statistical tests were performed using Prism software (Graphpad Software, San Diego, CA), and a value of $P < 0.05$ was considered significant. When necessary, nonlinear regression fitting was used to verify the trends in the time-course study. Student's *t*-test or ANOVA with Newman-Keuls posthoc test was used to determine the level of significance between the treatment groups.

RESULTS

Cholesterol homeostasis

In the control (without LXR agonist) experiments, total cholesterol (esterified and nonesterified) remained constant in both the HepG2 cells and the medium for the entire course of the study (96 h). However, in LXR agonist-treated cells, there was a reduction in cellular cholesterol from 56.8 ± 3.9 μg/mg cell protein at 24 h in the control group to 47.8 ± 1.7, 37.8 ± 0.5, 32.3 ± 2.0, and 31.4 ± 0.8 μg/mg cell protein in the GW3965-treated group at 24, 48, 72, and 96 h, respectively. Similar temporal decreases in cellular cholesterol were also observed in the T0901317 and SB742881 treatment groups (**Fig. 2A**). Consequently, there was an increase in the cell medium cholesterol concentration from 25.2 ± 1.7 μg/ml at 24 h in the control group to 28.0 ± 1.7, 33.3 ± 1.7, 34.0 ± 1.2, and 38.0 ± 01.7 μg/ml in the GW3965-treated group at 24, 48, 72, and 96 h, respectively. Similar temporal increases in medium cholesterol were also observed in the T0901317 and SB742881 groups (Fig. 2B). In contrast, there was no change in cellular cholesterol after treatment with 22(*R*)-hydroxycholesterol. However, cellular cholesterol decreased to 41.6 ± 2.2 and 36.5 ± 4.4 μg/mg cell protein after treatment with 24(*S*),25-epoxycholesterol and decreased to 49.0 ± 2.5 and 42.6 ± 5.2 μg/mg cell protein after treatment with DMHCA at 72 and 96 h, respectively (**Fig. 3A**). The medium cholesterol did not change significantly and remained ~35 μg/ml in the 22(*R*)-hydroxycholesterol-, 24(*S*),25-epoxycholesterol-, and DMHCA-treated groups (Fig. 3B).

Cellular free and esterified cholesterol pools were examined at 24 and 48 h to determine whether the different pools contributed to overall cholesterol handling by the cells. Both concentration (**Fig. 4A, C**) and ^{13}C enrichment (Fig. 4B, D) of cellular free cholesterol and cholesteryl esters were assessed at 24 and 48 h in control and GW3965-treated cells. Although the enrichment of esterified cholesterol was decreased initially at 24 h in the treated versus control cells, the enrichment of both free cholesterol and esterified cholesterol was higher in the treated versus

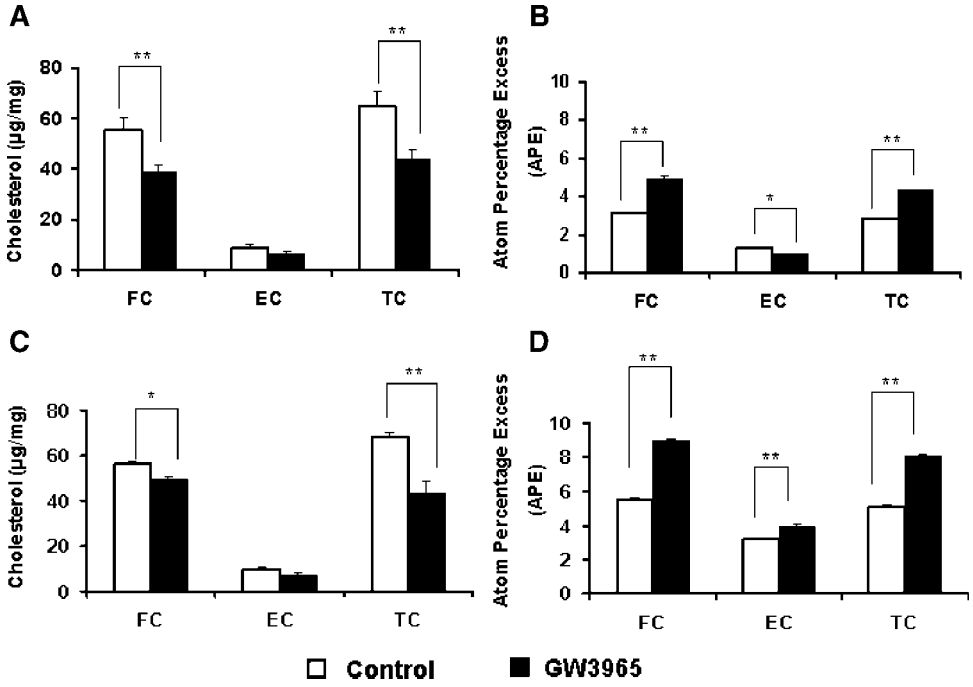

Fig. 4. Cellular free cholesterol (FC), esterified cholesterol (EC), and total cholesterol (TC) content and ^{13}C enrichment. The TLC-separated free and esterified cholesterol from 24 h-treated (A, B) and 48 h-treated (C, D) (GW3965, 1 μM or vehicle) HepG2 cells were analyzed using GC-MS. FC, EC, and TC contents are shown in A,C. FC, EC, and TC ^{13}C enrichment measured in atom percentage excess (APE) are shown in B, D. Data are presented as means ± SEM (n = 3). * $P < 0.01$, ** $P < 0.001$, control versus GW3965-treated groups.

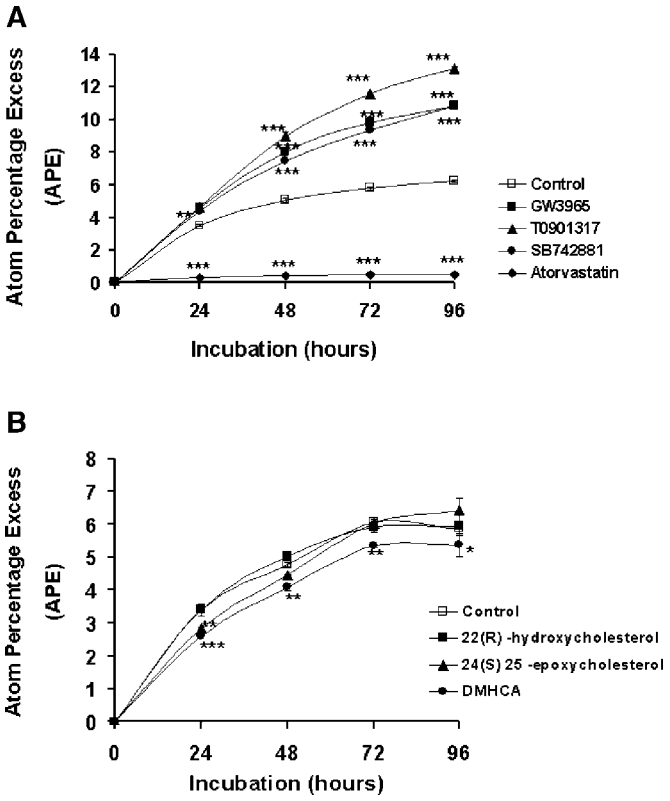

Fig. 5. Cellular cholesterol ^{13}C enrichment time course. Cellular cholesterol enrichment was measured in HepG2 cells during a 96 h incubation with GW3965 (1 μM), T0901317 (1 μM), SB742881 (1 μM), or atorvastatin (1 μM) (A) and 22(*R*)-hydroxycholesterol (1 μM), 24(*S*),25-epoxycholesterol (1 μM), or DMHCA (1 μM) (B). Data are presented as means ± SEM (n = 3). * $P < 0.05$, ** $P < 0.01$, *** $P < 0.001$, control versus treated groups.

control cells by 48 h (Fig. 4D). The total cholesterol pool and enrichment appear to reflect the rapid turnover of free cholesterol rather than the slow turnover of esterified cholesterol. Therefore, for the purposes of this study, kinetic modeling of the total cholesterol pool rather than separate free and esterified cholesterol pool modeling was performed.

Cholesterol ^{13}C labeling

To obtain kinetic data for mathematical modeling, [1-^{13}C]acetate precursor for cholesterol synthesis was added to HepG2 cells and [1-^{13}C]acetate incorporation into intracellular cholesterol after LXR treatment with two distinct structural classes; nonsteroidal and steroidal LXR agonists over a 96 h period were monitored (**Fig. 5**). The GW3965, T0901317, and SB742881 treatment groups showed an increase in the rate of cholesterol labeling, reflecting an increase in the rate of cholesterol synthesis (Fig. 5A). However, the natural LXR ligand [22(*R*)-hydroxycholesterol] had no effect on the rate of cholesterol labeling, whereas the steroidal LXR agonists [24(*S*),25-epoxycholesterol, DMHCA] appeared to slightly reduce the rate of cholesterol labeling, reflecting a decrease in the rate of cholesterol synthesis (Fig. 5B), consistent with earlier observations (6). Furthermore, as a positive control for the inhibition of cholesterol synthesis, a HMG-CoA reductase inhibitor (atorvastatin) was examined (Fig. 5A). A decrease in cholesterol synthesis in the atorvastatin-treated cells was consistent with the significantly lower cholesterol APE observed in these cells.

MIDA

A Monte Carlo simulation was used to generate the isotopomer distribution data for a given cholesterol precursor ^{13}C enrichment and for a given fraction of newly synthesized cholesterol. The cholesterol ^{13}C precursor enrichment percentage ($P = 45\%$) calculated in the present study was similar to two validated methods for measuring precursor enrichment: MIDA ($P = 47\%$) and isotopomer spectral analysis ($P = 49\%$). Although these methods estimate the precursor fractional ^{13}C enrichment differently, the underlying principle is the same. The calculated cholesterol precursor enrichment (p) and the percentage of newly synthesized cholesterol (f) for different treatment conditions at 24 h are shown in **Table 1**. The cholesterol precursor enrichment in the GW3965 group was increased rapidly and was stable throughout the study (37 ± 2%, 42 ± 1%, 43 ± 1%, and 45 ± 1% at 2, 4, 8, and 24 h, respectively). All treatment groups had similar precursor enrichments as their control groups at 24 h. The cholesterol precursor enrichment did not exceed 50% for the various experimental conditions when using [1-^{13}C]sodium acetate in the incubation medium, reflecting the steady state of the precursor pool. The newly synthesized cholesterol in HepG2 cells at 24 h increased from 19 ± 1% in the con-

TABLE 1. Percentage of precursor enrichment and newly synthesized cholesterol in HepG2 cells

Medium	Treatment	p	f
		%	
10% FBS	Control	45 ± 1	19 ± 1
10% FBS	GW3965	45 ± 0	28 ± 1[a]
10% FBS	T0901317	45 ± 1	26 ± 1[a]
10% FBS	SB742881	47 ± 2	24 ± 1[a]
10% FBS	Control	43 ± 2	17 ± 1
10% FBS	22(*R*)-Hydroxycholesterol	42 ± 1	18 ± 2
10% FBS	24(*S*),25-Epoxycholesterol	43 ± 1	15 ± 2
10% FBS	DMHCA	43 ± 0	14 ± 0[a]
Serum-free	Control	38 ± 1	28 ± 2
Serum-free	GW3965	38 ± 0	31 ± 1
Serum-free + apoA-I	Control	40 ± 0	22 ± 1
Serum-free + apoA-I	GW3965	38 ± 1	40 ± 0[a]
10% FBS	Control	40 ± 0	17 ± 1
10% FBS	Atorvastatin	40 ± 1	2 ± 0[a]

apoA-I, apolipoprotein A-I; DMHCA, *N,N*-dimethly-3β-hydroxycholenamide. The percentage of precursor enrichment (p) and the percentage of newly synthesized cholesterol (f) at 24 h for several studies using different culture conditions are shown. Precursor enrichment did not exceed 50% for the various experimental conditions using [1-^{13}C]sodium acetate in the incubation medium, reflecting a possible saturation of the precursor pool. Control for the GW3965, T0901317, and SB742881 studies was DMSO, control for the 22(*R*)-hydroxycholesterol, 24(*S*),25-epoxycholesterol, and DMHCA studies was ethanol, and control for the atorvastatin study was methanol. Data are presented as means ± SD.

[a] $P < 0.001$, control versus treated groups.

TABLE 2. Calculated cellular cholesterol fluxes for nonsteroidal LXR agonists

Treatment	U(1)	F(0,1)	F(1,2)	F(2,1)
		g/h/mg cell protein		
Control	0.15 ± 0.02	0.15 ± 0.02	2.89 ± 1.82	0.92 ± 0.15
GW3965 (24 h)	0.61 ± 0.03[a]	0.61 ± 0.01[a]	1.33 ± 0.11	2.46 ± 0.06[a]
GW3965 (48 h)	0.96 ± 0.02[a]	0.95 ± 0.0 1[a]	1.15 ± 0.14	1.93 ± 0.05[a]
GW3965 (72 h)	1.26 ± 0.04[a]	1.26 ± 0.01[a]	0.99 ± 0.09	1.69 ± 0.04[a]
GW3965 (96 h)	1.58 ± 0.04[a]	1.58 ± 0.02[a]	0.83 ± 0.11[b]	1.60 ± 0.04[a]
T0901317 (24 h)	0.60 ± 0.02[a]	0.28 ± 0.0 1[a]	1.39 ± 0.13	2.38 ± 0.17[a]
T0901317 (48 h)	0.94 ± 0.04[a]	0.43 ± 0.01[a]	1.10 ± 0.12	1.86 ± 0.13[a]
T0901317 (72 h)	1.24 ± 0.07[a]	0.57 ± 0.02[a]	0.81 ± 0.11[b]	1.64 ± 0.12[a]
T0901317 (96 h)	1.54 ± 0.06[a]	0.72 ± 0.02[a]	0.52 ± 0.12[b]	1.54 ± 0.11[a]
SB742881 (24 h)	0.62 ± 0.04[a]	0.15 ± 0.01	1.40 ± 0.30	2.69 ± 0.15[a]
SB742881 (48 h)	0.96 ± 0.06[a]	0.24 ± 0.01[a]	1.16 ± 0.32	2.11 ± 0.12[a]
SB742881 (72 h)	1.30 ± 0.08[a]	0.32 ± 0.02[a]	0.92 ± 0.30	1.85 ± 0.11[a]
SB742881 (96 h)	1.62 ± 0.12[a]	0.41 ± 0.02[a]	0.68 ± 0.34[b]	1.74 ± 0.10[a]
Atorvastatin	0.02 ± 0.01[a]	0.02 ± 0.01[a]	6.32 ± 3.21	1.56 ± 0.60

LXR, liver X receptor. The calculated cholesterol fluxes as predicted by the two-compartment kinetic model (Fig. 1) are shown. The notation F(destination, source) represents cholesterol flux as μg/h/mg cell protein. U(1) is the endogenous flux equivalent to the cholesterol synthesis flux. F(0,1) represents the cholesterol catabolic flux (i.e., bile acid synthesis, steroid synthesis, or other irreversible loss of cholesterol from the cells), F(1,2) represents the total cholesterol flux from the medium to the cells, and F(2,1) represents the total cholesterol flux from the cells to the medium. The control treatment was DMSO. Data are presented as means ± SD.

[a] $P < 0.01$, control versus treated groups.

[b] $P < 0.05$, control versus treated groups.

trol group to 28 ± 1%, 26 ± 1%, and 24 ± 1% ($P < 0.01$) after GW3965, T0901317, and SB742881 treatment, respectively, and decreased from 17 ± 1% to 2 ± 0% ($P < 0.001$) after atorvastatin treatment. However, newly synthesized cholesterol was not altered significantly [22(*R*)-hydroxycholesterol, 24(*S*),25-epoxycholesterol] or decreased (DMHCA) versus control at 24 h (Table 1). No significant differences were observed in the percentage of newly synthesized cholesterol under serum-free conditions.

Multicompartmental kinetic analysis

For the purpose of the multicompartment kinetic analysis, the influence of LXR agonists on HepG2 cells was assessed in experiments in which the medium contained serum. A two-compartment scheme representing total cholesterol in the cell (pool 1) and the medium (pool 2) was analyzed (Fig. 1). A steady-state fit was generated for the control, atorvastatin, and 22(*R*)-hydroxycholesterol treatment groups, as the cholesterol content in the cell and the medium remained constant. However, no steady-state solution was observed in the other LXR agonist treatment groups. Therefore, a transient fit was generated using the SAAM II software in which time dependence was embedded into the simulation with the observed cholesterol pool size in the cell and the medium compartments. The calculated fluxes (synthesis, catabolism, influx, efflux) at different incubation time points in the GW3965, T0901317, and SB742881 groups are presented in **Table 2**, and the 22(*R*)-hydroxycholesterol, 24(*S*),25-epoxycholesterol, and DMHCA group calculated fluxes are presented in **Table 3**. At 24 h, the synthesis of cholesterol in HepG2 cells increased from 0.15 ± 0.02 μg/h/mg cell protein in the control group to 0.61 ± 0.03, 0.60 ± 0.02, and 0.62 ± 0.04 μg/h/mg cell protein in the GW3965, T0901317, and SB742881 groups, respectively, and decreased to 0.02 ± 0.01 μg/h/mg cell protein in the atorvastatin group ($P <$ 0.01). Cholesterol influx at 24 h decreased from 2.89 ± 1.82 μg/h/mg cell protein in the control group to 1.33 ±

TABLE 3. Calculated cellular cholesterol fluxes for steroidal LXR agonists

Treatment	U(1)	F(0,1)	F(1,2)	F(2,1)
		g/h/mg cell protein		
Control	0.44 ± 0.12	0.44 ± 0.12	1.43 ± 0.40	1.39 ± 0.13
22(*R*)-Hydroxycholesterol	0.44 ± 0.00	0.44 ± 0.00	1.37 ± 0.16	1.40 ± 0.03
24(*S*),25-Epoxycholesterol (24 h)	0.27 ± 0.00[a]	0.33 ± 0.02	1.10 ± 0.02	1.09 ± 0.01[a]
24(*S*),25-Epoxycholesterol (48 h)	0.23 ± 0.00[a]	0.29 ± 0.02	0.97 ± 0.02	0.98 ± 0.02[a]
24(*S*),25-Epoxycholesterol (72 h)	0.21 ± 0.00[a]	0.26 ± 0.01[a]	0.85 ± 0.02[a]	0.87 ± 0.02[a]
24(*S*),25-Epoxycholesterol (96 h)	0.18 ± 0.01[a]	0.23 ± 0.01[a]	0.74 ± 0.03[a]	0.74 ± 0.01[a]
DMHCA (24 h)	0.32 ± 0.01	0.43 ± 0.05	0.93 ± 0.08	0.94 ± 0.06[a]
DMHCA (48 h)	0.30 ± 0.00[a]	0.40 ± 0.05	0.87 ± 0.06[a]	0.86 ± 0.02[a]
DMHCA (72 h)	0.28 ± 0.0[a]	0.36 ± 0.04	0.80 ± 0.05[a]	0.79 ± 0.04[a]
DMHCA (96 h)	0.25 ± 0.0[a]	0.33 ± 0.04	0.73 ± 0.06[a]	0.73 ± 0.05[a]

The calculated cholesterol fluxes as predicted by the two-compartment kinetic model (Fig. 1) are shown. The notation F(destination, source) represents cholesterol flux as μg/h/mg cell protein and is explained in Table 2. The control treatment was ethanol. Data are presented as means ± SD.

[a] $P < 0.05$, control versus treated groups.

0.11, 1.39 ± 0.13, and 1.40 ± 0.30 μg/h/mg cell protein in the GW3965, T0901317, and SB742881 groups, respectively, and increased to 6.32 ± 3.21 μg/h/mg cell protein in the atorvastatin group. The cholesterol efflux at 24 h increased from 0.92 ± 0.15 μg/h/mg cell protein in the control group to 2.46 ± 0.01, 2.38 ± 0.17, and 2.69 ± 0.15 μg/h/mg cell protein in the GW3965, T0901317, and SB742881 groups, respectively ($P < 0.01$), and increased to 1.56 ± 0.60 μg/h/mg cell protein in the atorvastatin group. Cholesterol fluxes in the steroidal LXR agonist treatment groups [22(*R*)-hydroxycholesterol, 24(*S*),25-epoxycholesterol, and DMHCA] were weakly modulated in contrast to the nonsteroidal LXR agonist treatment groups (GW3965, T0901317, and SB742881) (Table 3). Schematic representations of the effects of the different LXR agonists and of atorvastatin on cholesterol handling in HepG2 cells at 24 h are shown in **Fig. 6**.

Serum versus serum-free conditions

Cellular cholesterol flux responses were assessed in serum-free conditions to test whether any of the observed effects of the LXR agonist were attributable to the presence of serum components such as lipoproteins, which could serve as donors or acceptors of cellular cholesterol. In serum-free conditions, unlike in serum-containing conditions, there were no differences between control and GW3965-treated cells with regard to total cellular cholesterol content and cholesterol enrichment, suggesting that cholesterol handling after LXR activation is dependent on lipoproteins in serum (**Fig. 7A, B**). To further confirm the role of lipoproteins in the LXR activation of cholesterol efflux, GW3965-treated HepG2 cells were examined in the presence of apoA-I protein in serum-free medium. ApoA-I supplementation resulted in an increased cellular cholesterol enrichment versus control (Fig. 7B) but had no effect on cholesterol concentration (Fig. 7A). These data suggest that the increase in cholesterol enrichment observed with apoA-I supplementation is attributable to the increased turnover of cholesterol (increased synthesis and efflux) in this group in addition to the absence of a tracer dilution effect resulting from an influx of unlabeled cholesterol from the medium (Fig. 7B). Additionally, the potential contribution of apoB secretion by HepG2 cells to cholesterol efflux was examined by measuring the apoB concentration in the medium after treatment for 48 h with GW3965 at 1 μM. Treatment resulted in a slight, albeit nonsignificant, increase from 19.9 ± 1.4 to 22.2 ± 2.2 mg/dl/mg cell protein.

LXR gene expression

LXR activation of target gene expression was measured in control and GW3965, T0901317, and SB742881-treated HepG2 cells. These target genes included ABCA1 (cholesterol transported to lipid-poor lipoprotein A-I), ABCG1 (cholesterol transporter from lipid-loaded cells), FAS (integral to fatty acid biosynthesis), and SREBP1c (master transcription factor for lipogenic genes). The fold change in the expression of these genes after nonsteroidal LXR agonist treatment for 2, 4, 8, and 24 h is shown in **Fig. 8**. GW3965, T0901317, and SB742881 treatment resulted in a marked and temporal increase in ABCA1 expression by ~2-fold (Fig. 8A). ABCG1 expression was increased by at

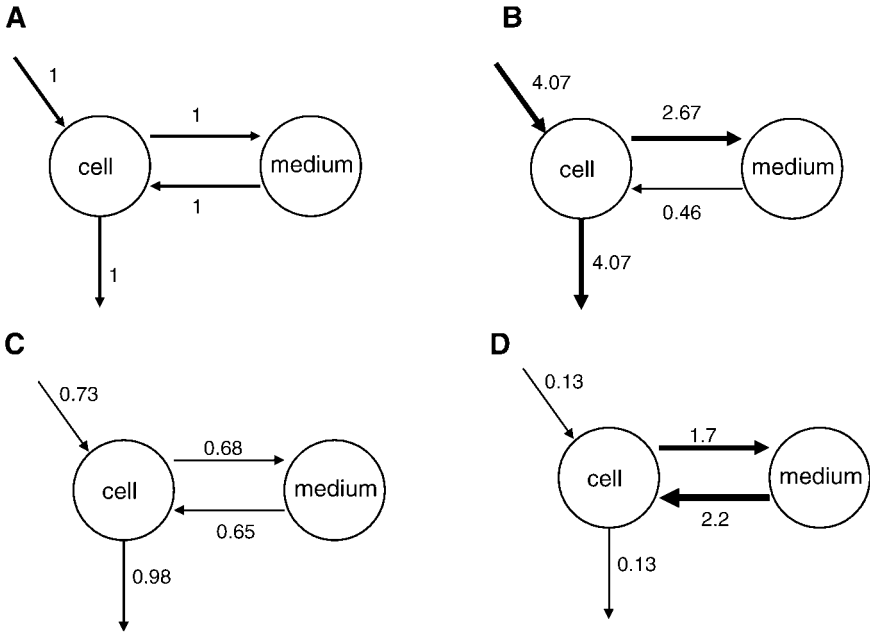

Fig. 6. Schemes of cholesterol flux handling after various treatments at 24 h. Shown are two-compartment analysis schematic representations of the control system (A), in which all fluxes are represented as unity, the nonsteroidal LXR agonist (GW3965) system (B), the steroidal LXR agonist (DMHCA) system (C), and the atorvastatin treatment system (D). System fluxes in B–D are presented as fold changes from the control system (A).

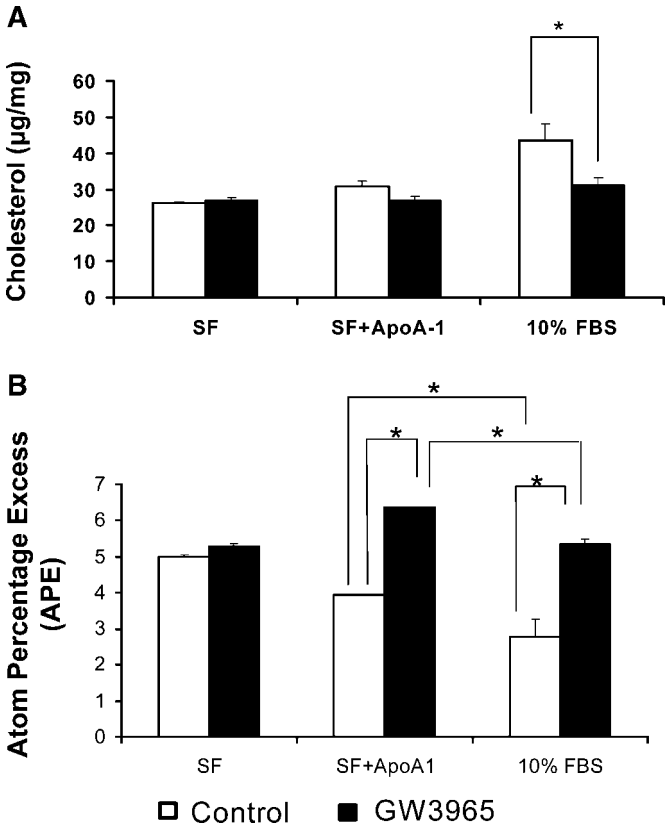

Fig. 7. Effect of cell culture medium composition on cellular cholesterol and ^{13}C enrichment in HepG2 cells. A: Cholesterol content in HepG2 cells in serum-free medium (SF), serum-free medium with apolipoprotein A-I (apoA-I) (SF+apoA-I), and culture medium with 10% FBS. B: Enrichment of cellular cholesterol in HepG2 cells in serum-free medium, serum-free medium with apoA-I, and culture medium with 10% FBS. See text for treatment conditions. Data are presented as means ± SEM (n = 3). * $P < 0.001$, control versus GW3965-treated groups.

least 100-fold at 24 h after GW3965, T0901317, and SB742881 treatment (Fig. 8B). FAS expression increased ~10-fold at 24 h after GW3965, T0901317, and SB742881 treatment (Fig. 8C). Finally, SREBP1c expression increased ~5-fold for the nonsteroidal LXR agonist treatment (Fig. 8D). The fold upregulation of the LXR-activated genes resulting from nonsteroidal LXR agonist (GW3965, T0901317, and SB742881) treatment appears to correlate with the LXRα EC_{50} of <300 nM for GW3965 (9), T0901317 (31), and SB742881 (unpublished data). The cholesterol flux measurements also appear to correlate with LXR gene activation.

Additional genes that are associated with various cellular cholesterol flux pathways (e.g., HMG-CoA reductase and SREBP2 for cholesterol synthesis, LDLR and SR-BI for cellular cholesterol flux, and CYP7A1 for bile acid synthesis) were examined in HepG2 cells treated with GW3965 for 24 h. HMG-CoA reductase and SREBP2 expression was increased by 3.0 ± 0.5-fold and 1.9 ± 0.1-fold ($P < 0.001$), respectively, after treatment and was consistent with the increased cholesterol synthesis observed in treated cells. SR-BI expression was increased by 1.6 ± 0.2-fold ($P < 0.001$) after treatment and was consistent with the increased cholesterol efflux observed in treated cells. LDLR expression was increased by 3.2 ± 0.4-fold ($P < 0.001$) after treatment and may reflect the cell's activation of cholesterol transport machinery in an attempt to maintain cellular cholesterol homeostasis. However, there was no change in CYP7A1 expression after treatment.

DISCUSSION

A multicompartment kinetic analysis was used to examine the effects of two structurally distinct LXR agonists: nonsteroidal LXR agonists (GW3965, T0901317, and SB742881) and steroidal LXR agonists [22(*R*)-hydroxycholesterol, 24(*S*),25-epoxycholesterol, and DMHCA] on cellular cholesterol handling in HepG2 cells. Consistent with the LXR activation of reverse cholesterol transport, there was a significant decrease in cellular cholesterol content and a corresponding increase in cholesterol content in the cell culture medium after HepG2 cell treatment with these compounds. However, there was a clear distinction between potent nonsteroidal synthetic activators (GW3965, T0901317, and SB742881) and low-potency steroidal LXR activators [22(*R*)-hydroxycholesterol, 24(*S*),25-epoxycholesterol, and DMHCA] in cellular cholesterol handling. The reason for the differences may be attributable to the differences in LXRα EC_{50}, which is ~300 nM for the synthetic, nonsteroidal LXR agonists versus ~3 µM for the natural and synthetic steroidal LXR agonists (32). The decrease in cellular cholesterol content in nonsteroidal LXR agonist-treated HepG2 cells was associated with an increase in cellular cholesterol efflux F(2,1) and a decrease in cellular cholesterol influx F(1,2) by 96 h. In response to the increased cholesterol efflux associated with the potent LXR agonists, it is likely that cholesterol synthesis U(1) was increased as a compensatory means of maintaining cellular cholesterol levels. However, the increased cholesterol catabolic flux F(0,1) after nonsteroidal LXR activation could not be attributed to any major bile acids (cholic or chenodeoxycholic acid) or its precursor (7α-hydroxy-cholestenone) in this study (data not shown). The loss of some precursor intermediates, such as desmosterol and lathosterol (33, 34), into culture medium also cannot explain the increase in F(0,1) observed in our study, as the levels of these sterols are typically extremely low (<200 ng/ml) in the culture medium analyzed. Therefore, flux F(0,1) represents an irreversible loss of cholesterol into medium, possibly as other undetermined neutral sterols. These studies, for the first time, have allowed for the comprehensive assessment of cholesterol handling (i.e., synthesis, catabolism, influx, and efflux) after LXR activation.

To fully appreciate the interpretation of the mathematical modeling of cholesterol flux, one has to take into consideration the potential for multiple intracellular cholesterol compartments to exist and for these subcompartments to turn over at different rates. Varying degrees of cholesterol exchange between the plasma membrane and

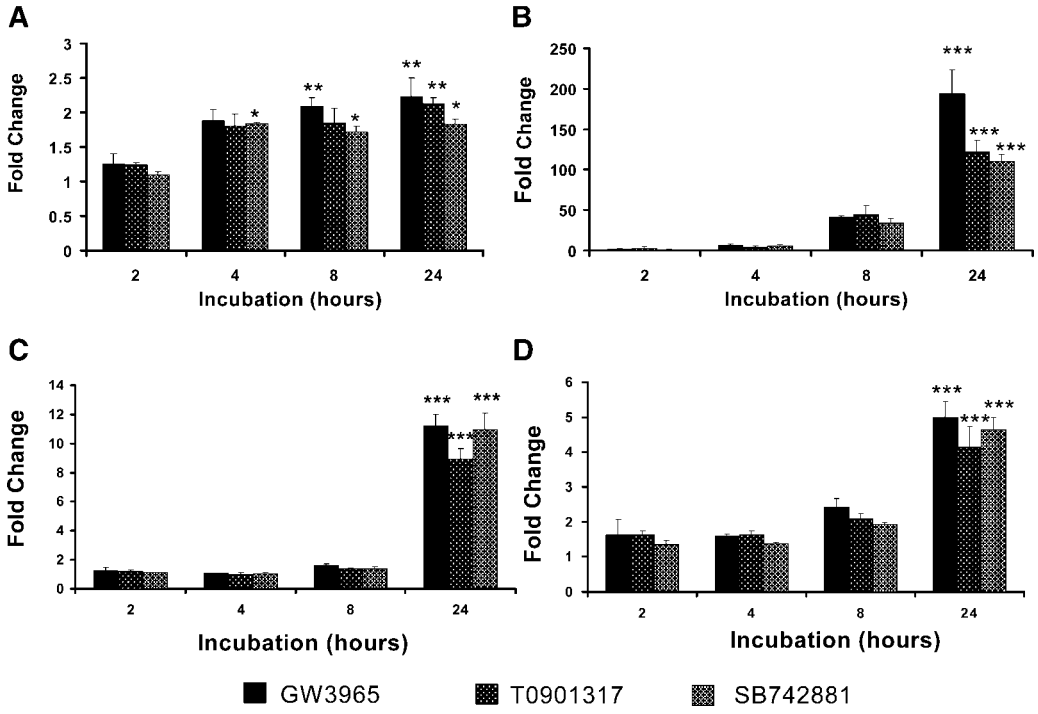

Fig. 8. LXR-activated gene expression time course in HepG2 cells after nonsteroidal LXR agonist treatment. ABCA1 (A), ABCG1 (B), FAS (C), and sterol-regulatory element binding protein 1c (D) gene expression in GW3965-, T0901317-, and SB742881-treated HepG2 cells. Cells were treated with 1 μM of each of the nonsteroidal LXR agonists. Data are represented as fold change from the control at a given time point. Data are presented as means ± SEM (n = 4). * $P < 0.05$, ** $P < 0.01$, *** $P < 0.001$, control versus treated groups.

intracellular compartments, and higher cholesterol enrichments observed in the lysosome and endoplasmic reticulum than in the plasma membrane of cells when labeled with [^{14}C]acetate or with [^{14}C]free cholesterol-LDL (35, 36), suggest cholesterol subcompartments in the cell. In the modeling scheme used in this study, the use of exchangeable cholesterol pool sizes eliminated the need for complex subcellular modeling in terms of free and esterified cholesterol. The calculated nonexchangeable cholesterol fraction agrees with the fraction of cholesterol in the plasma membrane, which is considered to be more cholesterol-rich than other intracellular membranes (37). Although most of the cholesterol in the cell (~60–80%) is found in the plasma membrane, it is considered to be much less sensitive than the endoplasmic reticulum cholesterol pool (~1%) to perturbation in cholesterol content; therefore, it is consistent with the hypothesis that intracellular cholesterol trafficking is the rate-limiting step in regulating cholesterol efflux (38).

By using an exchangeable cellular cholesterol pool size, the current model analysis avoids the need for complex compartmental modeling of the subcellular cholesterol fraction. Using the actual cholesterol content in cells and in the medium over the 96 h treatment period for GW3965, T0901317, and SB742881 generated the best fit for this non-steady-state model. The model presented here is a cumulative linear model and does not consider the time-dependent effects of the actual concentration of the acetate precursor and treatment compounds, which would require a nonlinear, noncumulative approach and is beyond the scope of this study. Thus, we have avoided a complex modeling scheme (39) and tedious multiple labeling studies (11) to obtain a reliable parameter estimation.

The precursor ^{13}C enrichment and percentage fractional synthesis of cholesterol in the control group as calculated by MIDA were comparable to those published previously (11, 12). Additionally, we examined the dynamic fidelity of the mathematical model with regard to cholesterol handling using atorvastatin, a HMG-CoA reductase inhibitor. A dramatic reduction in cholesterol APE was observed at 24 to 96 h compared with the control group (Fig. 5). This observed reduction in cholesterol enrichment was attributable to the rapid decline of labeled species entering the cholesterol biosynthesis pathway as well as to possible product dilution from the increased cellular uptake of unlabeled LDL cholesterol by upregulation of the LDLR. Although the calculated cholesterol precursor enrichment (p) of 40% was similar to that in the other groups, the percentage of newly synthesized cholesterol (f) varied dramatically (2%, 24–28%, and 14–18% for atorvastatin, nonsteroidal LXR agonists, and steroidal LXR agonists, respectively).

A 1 day stable isotope study was performed to examine the relationship between cholesterol labeling at 2, 4, 8, and 24 h (data not shown) and gene expression at these time points. During the first 8 h of treatment, there was no difference in the enrichment of cholesterol between the

control and GW3965 treatment groups, consistent with activation of the gene expression profile. Significant upregulation of ABCA1, ABCG1, FAS, and SREBP1c in HepG2 cells was observed within 24 h of treatment with GW3965, T0901317, and SB742881. The cholesterol enrichment after strong LXR activation in HepG2 cells temporally correlated with the activation of these genes and cholesterol synthesis.

The increased cholesterol efflux from HepG2 cells appeared to be the result of the combined effects of ABCA1- and ABCG1-mediated efflux to the regulatory proteins apoA-I and HDL, respectively (40, 41), and not of apoB-mediated cholesterol efflux by the cells, because no significant change was observed in apoB secretion after treatment with GW3965. As a consequence of the upregulation of these genes, cellular cholesterol efflux to acceptors in serum or to exogenously added apoA-I was stimulated, resulting in a decrease in intracellular cholesterol content and a compensatory increase in cholesterol synthesis (Table 1) as a means of maintaining cholesterol homeostasis. These responses vanished when the medium was deprived of serum. After treatment with GW3965, T0901317, or SB742881, the cell makes available both the plasma membrane and endoplasmic reticulum cholesterol for efflux. A decrease in endoplasmic reticulum cholesterol may result in the upregulation of cholesterol synthesis, presumably through the activation of SREBP2 (42). Indeed, upregulation of SREBP2 (~2-fold) was observed in GW3965-treated cells by 24 h. It was shown previously that cholesterol biosynthesis and efflux are stimulated in HepG2 cells expressing caveolin-I as a result of a decrease in endoplasmic reticulum cholesterol and an enhanced transfer of intracellular cholesterol to cholesterol-rich domains in the plasma membrane, respectively (43). Although the physiological function of ABCG1 in macrophage foam cells is well established (44, 45), its role in liver cells is not well understood. Overexpression of ABCG1 in mouse liver resulted in increased biliary excretion of cholesterol and decreased plasma HDL levels in vivo (46). However, although potent ABCG1 upregulation by GW3965, T0901317, and SB742881 in HepG2 cells was observed, bile acid precursor or products were not detected in the cell or medium in this study (data not shown). This finding was consistent with the lack of activation of the CYP7A1 gene by GW3965 in this study, consistent with the fact that the human CYP7A1 gene does not have an LXR response element (47).

In summary, the major advantages of the two-compartment system investigated here are that it is identifiable and distinguishable (48) and it allows for the simultaneous investigation of the whole cell system without any external assumptions. The results from this statistical and multicompartment modeling approach not only provided a biological interpretation of cholesterol handling but also provided some insight into the comprehensive cholesterol handling after potent and weak LXR activation (Fig. 6). In this respect, the increase in the percentage of newly synthesized cholesterol after potent LXR activation (GW3965, T0901317, and SB742881) may be secondary to the increase in cholesterol efflux. The model presented here could be used to obtain flux profiles of cholesterol handling after treatment with drugs and can be extended to additional cell types in which cholesterol fluxes are modulated.

The authors thank John Krawiec and Sara Pilar Alom Ruiz for helping us with gene expression studies, Chad Quinn for GC-MS support and helpful advice, and Harvey Fries and Christopher Evans for LXR agonist concentration and bile acid analysis.

REFERENCES

1. Jaye, M. 2003. LXR agonists for the treatment of atherosclerosis. *Curr. Opin. Investig. Drugs.* **4:** 1053–1058.
2. Tontonoz, P., and D. J. Mangelsdorf. 2003. Liver X receptor signaling pathways in cardiovascular disease. *Mol. Endocrinol.* **17:** 985–993.
3. Repa, J. J., and D. J. Mangelsdorf. 2002. The liver X receptor gene team: potential new players in atherosclerosis. *Nat. Med.* **8:** 1243–1248.
4. Sparrow, C. P., J. Baffic, M. H. Lam, E. G. Lund, A. D. Adams, X. Fu, N. Hayes, A. B. Jones, K. L. MacNaul, J. Ondeyka, et al. 2002. A potent synthetic LXR agonist is more effective than cholesterol loading at inducing ABCA1 mRNA and stimulating cholesterol efflux. *J. Biol. Chem.* **277:** 10021–10027.
5. Plösch, T., T. Kok, V. W. Bloks, M. J. Smit, R. Haringa, G. Chimini, A. K. Groen, and F. Kuipers. 2002. Increased hepatobiliary and fecal cholesterol excretion upon activation of the liver X receptor is independent of ABCA1. *J. Biol. Chem.* **277:** 33870–33877.
6. Schroepfer, G. J., Jr. 2000. Oxysterols: modulators of cholesterol metabolism and other processes. *Physiol. Rev.* **80:** 361–554.
7. Janowski, B. A., P. J. Willy, T. R. Devi, J. R. Falck, and D. J. Mangelsdorf. 1996. An oxysterol signalling pathway mediated by the nuclear receptor LXR alpha. *Nature.* **383:** 728–731.
8. Fu, X., J. G. Menke, Y. Chen, G. Zhou, K. L. MacNaul, S. D. Wright, C. P. Sparrow, and E. Lund. 2001. 27-Hydroxycholesterol is an endogenous ligand for liver X receptor in cholesterol-loaded cells. *J. Biol. Chem.* **276:** 38378–38387.
9. Joseph, S. B., E. McKilligin, L. Pei, M. A. Watson, A. R. Collins, B. A. Laffitte, M. Chen, G. Noh, J. Goodman, G. N. Hagger, et al. 2002. Synthetic LXR ligand inhibits the development of atherosclerosis in mice. *Proc. Natl. Acad. Sci. USA.* **99:** 7604–7609.
10. Schultz, J. R., H. Tu, A. Luk, J. J. Repa, J. C. Medina, L. Li, S. Schwendener, S. Wang, M. Thoolen, D. J. Mangelsdorf, et al. 2000. Role of LXRs in control of lipogenesis. *Genes Dev.* **14:** 2831–2838.
11. Holleran, A. L., B. Lindenthal, T. A. Aldaghlas, and J. K. Kelleher. 1998. Effect of tamoxifen on cholesterol synthesis in HepG2 cells and cultured rat hepatocytes. *Metabolism.* **47:** 1504–1513.
12. Kelleher, J. K., A. T. Kharroubi, T. A. Aldaghlas, I. B. Shambat, K. A. Kennedy, A. L. Holleran, and T. M. Masterson. 1994. Isotopomer spectral analysis of cholesterol synthesis: applications in human hepatoma cells. *Am. J. Physiol.* **266:** E384–E395.
13. Sniderman, A. D., Z. Zhang, J. Genest, and K. Cianflone. 2003. Effects on apoB-100 secretion and bile acid synthesis by redirecting cholesterol efflux from HepG2 cells. *J. Lipid Res.* **44:** 527–532.
14. Levy, J., K. Budai, and N. B. Javitt. 1994. Bile acid synthesis in HepG2 cells: effect of cyclosporine. *J. Lipid Res.* **35:** 1795–1800.
15. Brissette, L., M. C. Charest, L. Falstrault, J. Lafond, D. Rhainds, C. Tremblay, and T. Q. Truong. 1999. Selective uptake of cholesteryl esters from various classes of lipoproteins by HepG2 cells. *Biochem. Cell Biol.* **77:** 157–163.
16. Xu, X. X., and I. Tabas. 1991. Lipoproteins activate acyl-coenzyme A:cholesterol acyltransferase in macrophages only after cellular cholesterol pools are expanded to a critical threshold level. *J. Biol. Chem.* **266:** 17040–17048.
17. Phillips, M. C., W. J. Johnson, and G. H. Rothblat. 1987. Mechanisms and consequences of cellular cholesterol exchange and transfer. *Biochim. Biophys. Acta.* **966:** 223–276.
18. Czarnecka, H., and S. Yokoyama. 1996. Regulation of cellular cholesterol efflux by lecithin:cholesterol acyltransferase reaction through nonspecific lipid exchange. *J. Biol. Chem.* **271:** 2023–2028.
19. Johnson, W. J., F. H. Manlberg, G. K. Chacka, M. C. Phillips, and G. H. Rothblat. 1988. The influence of cellular and lipoprotein cholesterol contents on the flux of cholesterol between fibroblasts and high density lipoprotein. *J. Biol. Chem.* **263:** 14099–14106.

20. Sviridov, D., L. E. Pyle, and N. Fidge. 1996. Efflux of cellular cholesterol and phospholipid to apolipoprotein A-I mutants. *J. Biol. Chem.* **271:** 33277–33283.
21. Javitt, N. B. 1990. Hep G2 cells as a resource for metabolic studies: lipoprotein, cholesterol, and bile acids. *FASEB J.* **4:** 161–168.
22. Dixon, J. L., and H. N. Ginsberg. 1993. Regulation of hepatic secretion of apolipoprotein B-containing lipoproteins: information obtained from cultured liver cells. *J. Lipid Res.* **34:** 167–179.
23. Einarsson, C., E. Ellis, A. Abrahamsson, B. Ericzon, I. Bjorkhem, and M. Axelson. 2000. Bile acid formation in primary human hepatocytes. *World J. Gastroenterol.* **6:** 522–525.
24. Hellerstein, M. K., and R. A. Neese. 1992. Mass isotopomer distribution analysis: a technique for measuring biosynthesis and turnover of polymers. *Am. J. Physiol.* **263:** E988–E1001.
25. Hellerstein, M. K., C. Kletke, S. Kaempfer, K. Wu, and C. H. Shackleton. 1991. Use of mass isotopomer distributions in secreted lipids to sample lipogenic acetyl-CoA pool in vivo in humans. *Am. J. Physiol.* **261:** E479–E486.
26. Batta, A. K., G. Salen, P. Batta, G. S. Tint, D. S. Alberts, and D. L. Earnest. 2002. Simultaneous quantitation of fatty acids, sterols and bile acids in human stool by capillary gas-liquid chromatography. *J. Chromatogr. B.* **775:** 153–161.
27. Hellerstein, M. K., and R. A. Neese. 1999. Mass isotopomer distribution analysis at eight years: theoretical, analytic, and experimental considerations. *Am. J. Physiol.* **276:** E1146–E1170.
28. Pont, F., L. Duvillard, B. Verges, and P. Gambert. 1998. Development of compartmental models in stable-isotope experiments: application to lipid metabolism. *Arterioscler. Thromb. Vasc. Biol.* **18:** 853–860.
29. Millar, J. S., A. H. Lichtenstein, G. G. Dolnikowski, J. M. Ordovas, and E. J. Schaefer. 1998. Proposal of a multicompartmental model for use in the study of apolipoprotein E metabolism. *Metabolism.* **47:** 922–928.
30. Branswig, S., A. Kerksiek, T. Sudhop, C. Luers, K. V. Bergmann, and H. K. Berthod. 2002. Carbamazepine increases atherogenic lipoproteins: mechanism of action in male adults. *Am. J. Physiol.* **282:** H704–H716.
31. Repa, J. J., S. D. Turley, J. M. A. Lobaccaro, J. Medina, L. Li, K. Lustig, B. Shan, R. A. Heyman, J. M. Dietschy, and D. J. Mangelsdorf. 2000. Regulation of absorption and ABC1-mediated efflux of cholesterol by RXR heterodimers. *Science.* **289:** 1524–1529.
32. Janowski, B. A., M. J. Grogan, S. A. Jones, G. B. Wisely, S. A. Kliewer, E. J. Corey, and D. J. Mangelsdorf. 1999. Structural requirements of ligands for the oxysterol liver X receptors LXRalpha and LXRbeta. *Proc. Natl. Acad. Sci. USA.* **96:** 266–271.
33. Phillips, J. E., W. V. Rodrigueza, and W. J. Johnson. 1998. Basis for rapid efflux of biosynthetic desmosterol from cells. *J. Lipid Res.* **39:** 2459–2470.
34. Lusa, S., S. Heino, and E. Ikonen. 2003. Differential mobilization of newly synthesized cholesterol and biosynthetic sterol precursors from cells. *J. Biol. Chem.* **278:** 19844–19851.
35. Wustner, D., A. Herrman, M. Hao, and F. R. Maxfield. 2002. Rapid nonvesicular transport of sterol between the plasma membrane domains of polarized hepatic cells. *J. Biol. Chem.* **277:** 30325–30336.
36. Sviridov, D., and N. Fidge. 1995. Efflux of intracellular versus plasma membrane cholesterol in HepG2 cells: different availability and regulation by apolipoprotein A-I. *J. Lipid Res.* **36:** 1887–1896.
37. Maxfield, F. R., and D. Wustner. 2002. Intracellular cholesterol transport. *J. Clin. Invest.* **110:** 891–898.
38. Oram, J. F., A. J. Mendez, J. P. Slotte, and T. F. Johnson. 1991. High density lipoprotein apolipoproteins mediate removal of sterol from intracellular pools but not from plasma membranes of cholesterol-loaded fibroblasts. *Arterioscler. Thromb.* **11:** 403–414.
39. Guas, K., J. J. Gooding, R. T. Dean, L. Kritharides, and W. Jessup. 2001. A kinetic model to evaluate cholesterol efflux from THP-1 macrophages to apolipoprotein A-1. *Biochemistry.* **40:** 9363–9373.
40. Wang, N., D. L. Silver, C. Thiele, and A. R. Tall. 2001. ATP-binding cassette transporter A1 (ABCA1) functions as a cholesterol efflux regulatory protein. *J. Biol. Chem.* **276:** 23742–23747.
41. Kennedy, M. A., G. C. Barrera, K. Nakamura, A. Baldan, P. Tarr, M. C. Fishbein, J. Frank, O. L. Francone, and P. A. Edwards. 2005. ABCG1 has a critical role in mediating cholesterol efflux to HDL and preventing cellular lipid accumulation. *Cell Metab.* **1:** 121–131.
42. Basso, F., L. Freeman, C. L. Knapper, A. Remaley, J. Stonik, E. B. Neufeld, T. Tansey, M. J. Amar, J. F. Najib, N. Duverger, et al. 2003. Role of the hepatic ABCA1 transporter in modulating intrahepatic cholesterol and plasma HDL cholesterol concentrations. *J. Lipid Res.* **44:** 296–302.
43. Fu, Y., A. Hoang, G. Escher, R. G. Parton, Z. Krozowski, and D. Sviridov. 2004. Expression of caveolin-1 enhances cholesterol efflux in hepatic cells. *J. Biol. Chem.* **279:** 14140–14146.
44. Gelissen, I. C., M. Harris, K. A. Rye, C. Quinn, A. J. Brow, M. Kockx, S. Cartland, M. Packianathan, L. Kritharides, and W. Jessup. 2006. ABCA1 and ABCG1 synergize to mediate cholesterol export to apoA-1. *Arterioscler. Thromb. Vasc. Biol.* **26:** 534–540.
45. Schmitz, G., T. Langmann, and S. Heimerl. 2001. Role of ABCG1 and other ABCG family members in lipid metabolism. *J. Lipid Res.* **42:** 1513–1520.
46. Ito, T. 2003. Physiological function of ABCG1. *Drug News Perspect.* **16:** 490–492.
47. Chaing, J. Y., R. Kimmel, and D. Stroup. 2001. Regulation of cholesterol 7alpha-hydroxylase gene (CYP7A1) transcription by the liver orphan receptor (LXRalpha). *Gene.* **262:** 257–265.
48. Cobelli, C., D. Foster, and G. Tofolo. 2000. Tracer Kinetics in Biomedical Research: From Data to Model. Kluwer Academic Publishers, New York.